

Silole-Containing Polymers for High-Efficiency Polymer Solar Cells

Jinsheng Song,^{1,2} Chun Du,¹ Cuihong Li,² Zhishan Bo^{1,2}

¹Institute of Polymer Chemistry and Physics, College of Chemistry, Beijing Normal University, Beijing 100875, China

²Laboratory of Polymer Physics and Chemistry, Institute of Chemistry, Chinese Academy of Sciences, Beijing 100190, China

Correspondence to: Z. Bo (E-mail: zsbo@iccas.ac.cn)

Received 21 March 2011; accepted 30 June 2011; published online 28 July 2011

DOI: 10.1002/pola.24870

ABSTRACT: Silole-containing conjugated polymers (**P1** and **P2**) carrying methyl and octyl substituents, respectively, on the silicon atom were synthesized by Suzuki polycondensation. They show strong absorption in the region of 300–700 nm with a band gap of about 1.9 eV. The two silole-containing conjugated polymers were used to fabricate polymer solar cells by blending with PC₆₁BM and PC₇₁BM as the active layer. The best performance of photovoltaic devices based on **P1**/PC₇₁BM active layer exhibited power conversion efficiency (PCE) of 2.72%, whereas that of the photovoltaic cells fabricated with **P2**/

PC₇₁BM exhibited PCE of 5.08%. 1,8-Diiodooctane was used as an additive to adjust the morphology of the active layer during the device optimization. PCE of devices based on **P2**/PC₇₁BM was further improved to 6.05% when a TiO_x layer was used as a hole-blocking layer. © 2011 Wiley Periodicals, Inc. *J Polym Sci Part A: Polym Chem* 49: 4267–4274, 2011

KEYWORDS: benzo[*c*][1,2,5]thiadiazole; conjugated polymers; donor materials; fullerenes; hole-blocking layer; polymer solar cells; silole; spin coating

INTRODUCTION Polymer solar cells (PSCs) have attracted considerable attention due to their advantages such as low cost, light weight, and easy processing. Recently, power conversion efficiency (PCE) higher than 7%^{1,2} has been reported for PSCs and lots of research results have shown that both the material design and device fabrication process played important roles in achieving high photovoltaic performances. Except poly(3-hexylthiophene)s, high PCE polymer donor materials usually have a common feature of main chain donor acceptor alternating structure.^{3–12} And properties of polymer materials such as energy level, absorption spectrum, and solubility can be easily tuned by changing structures of donor and acceptor repeating units.

Silole-containing aromatic units have recently been investigated as novel building blocks for conjugated polymer materials, because the σ^* -orbital of the silicon–carbon bond can effectively interact with the π^* -orbital of the butadiene fragment, leading to a lowest unoccupied molecular orbital (LUMO) energy level. Silole-containing conjugated polymers have been widely used in the field of organic light-emitting diodes¹³ and field-effect transistors (FETs),¹⁴ since the report that 2,5-di(2-pyridyl)silole derivatives exhibit promising electron-transporting properties by Tamao et al.¹⁵ Recently, Cao's and Yang's group have applied silole-containing polymers in the fabrication of polymer photovoltaic cells and PCEs higher than 5% have been reached.^{16,4} Very

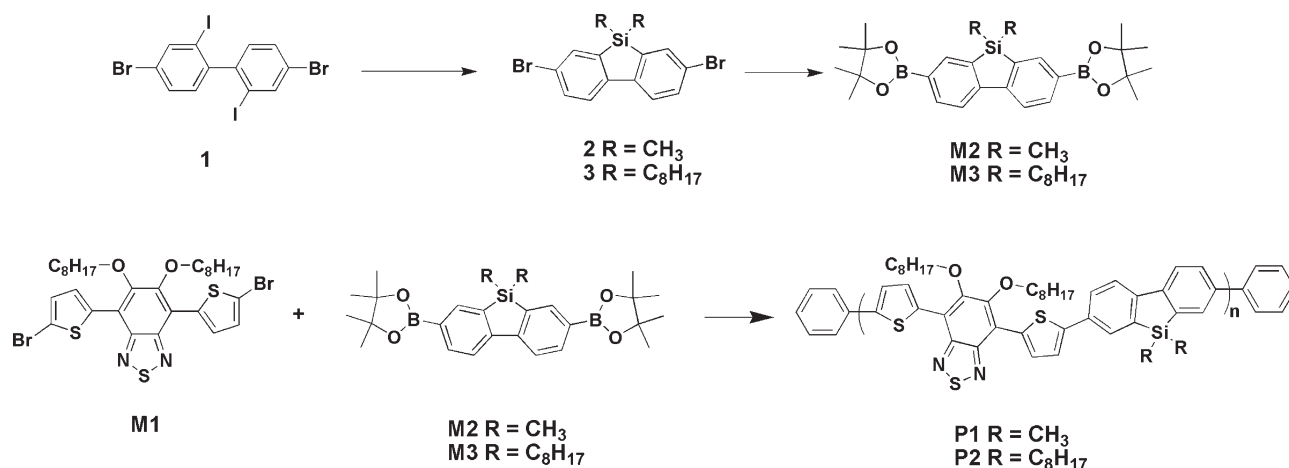
recently, Scharber's and Yang's groups have also indicated replacing the carbon by a silicon can obtain a smaller distortion for the conjugated polymer backbone, which will lead to a better packing of polymer chains.^{12,9}

Benzothiadiazole is a promising building block for donor materials used in PSCs, which exhibit higher PCE. In practice, because of their limited solubility, many benzothiadiazole-based polymers are of lower molecular weight. We have found that the attaching of two flexible alkoxy chains on benzothiadiazole unit can significantly increase their copolymers' solubility without significant influence on their energy levels. In our previous article, we have reported that PSCs based on benzothiadiazole-containing copolymers, poly(2-(5-(5,6-bis(octyloxy)-4-(thiophen-2-yl)benzo[*c*][1,2,5]thiadiazol-7-yl)thiophen-2-yl)-9-octyl-9*H*-carbazole), showed a PCE of 5.4%.⁸ The introduction of two flexible alkoxy chains onto the benzothiadiazole can significantly increase the solubility of polymers without drastically decreasing the planarity of polymer main chains.⁸

In this article, two new kinds of copolymers poly(4-(5-(9,9-dimethyl-9*H*-dibenzosilole-2-yl)thiophen-2-yl)-5,6-bis(octyloxy)-7-(thiophen-2-yl)benzo[*c*][1,2,5]thiadiazole) (**P1**) and poly(4-(5-(9,9-dioctyl-9*H*-dibenzosilole-2-yl)thiophen-2-yl)-5,6-bis(octyloxy)-7-(thiophen-2-yl)benzo[*c*][1,2,5]thiadiazole) (**P2**) were designed, synthesized, and used in solar cell device fabrication. The average performance of five solar cells based on **P2**

Additional Supporting Information may be found in the online version of this article.

© 2011 Wiley Periodicals, Inc.

SCHEME 1 Synthesis of **P1** and **P2**.

blended with PC₇₁BM illustrated a short current density (J_{sc}) of 10.67 mA cm⁻², an open-circuit voltage (V_{oc}) of 0.84 V, a fill factor (FF) of 0.59, and a PCE of 5.08% under air mass (AM) 1.5 (100 mW cm⁻²). When TiO_x was used as an electron-blocking layer, the photovoltaic performance was greatly improved and the PCE increased to 6.05% (V_{oc} = 0.91 V, J_{sc} = 11.5 mA cm⁻², and FF = 0.58), making **P2** a very promising polymer for solar cell application.

RESULTS AND DISCUSSION

The synthesis of **P1** and **P2** is shown in Scheme 1. Starting from 4,4'-dibromo-2,2'-diiodobiphenyl (**1**), the treatment of Compound **1** with 4 equiv of *n*-BuLi in tetrahydrofuran (THF) was followed by quenching with dichlorodimethylsilane affording 2,7-dibromo-9,9-dimethyldibenzosilole (**2**) in a yield of 40%. Miyaura cross-coupling of **2** and bis(pinacolato)diboron with Pd(dppf)₂Cl₂ as the catalyst precursor afforded 9,9-dimethyl-2,7-bis(4,4,5,5-tetramethyl-1,3,2-dioxaborolane-2-yl)dibenzosilole (**M2**) in a yield of 75%. 4,7-Bis(5-bromothiophen-2-yl)-5,6-bis(octyloxy)benzo[*c*][1,2,5]-thiadiazole⁸ (**M1**) and 9,9-dioctyl-2,7-bis(4,4,5,5-tetramethyl-1,3,2-dioxaborolane-2-yl)dibenzosilole^{13,17} (**M3**) were prepared according to literature procedures. Suzuki–Miyaura–Schlüter polycondensation was carried out in a biphasic mixture of THF/toluene (1:3)/aqueous NaHCO₃ with Pd(PPh₃)₄ as the catalyst precursor. Polymers **P1** and **P2** were obtained as dark red solid in yields of 84 and 90%, respectively.

Molecular Weights and Thermal Properties

Both polymers displayed good solubility in chloroform, chlorobenzene (CB), 1,2-dichlorobenzene (DCB), THF and so forth at room temperature. Molecular weights and polydispersity indexes (PDIs) of the polymers were determined by gel permeation chromatography (GPC) against polystyrene standards with THF as an eluent. Number-average molecular weights (M_n) of 79.8 and 102 kg mol⁻¹ were obtained for **P1** and **P2** with PDI of 1.46 and 1.66, respectively. Thermogravimetric analysis (TGA) studies revealed that both the two polymers are stable up to ~330 °C. Glass transition temperatures of **P1** and **P2** were determined by differential scanning

calorimetry (DSC) at a heating and cooling speed of 20 °C min⁻¹ to be 134.6 and 136.8 °C, respectively.

Electrochemical and Optical Properties

The electrochemical properties of **P1** and **P2** were investigated by cyclic voltammetry (CV) with a standard three-electrode electrochemical cell in a 0.1-M tetrabutylammonium hexafluorophosphate solution in acetonitrile at room temperature under a nitrogen atmosphere with a scanning rate of 100 mV s⁻¹. Ag/AgNO₃ was used as the reference electrode and a standard ferrocene/ferrocenium redox system was used as the internal standard. The CV curves of **P1** and **P2** are shown in Figure 1. The onset oxidation potentials (E_{ox}) are 0.62 and 0.73 V for **P1** and **P2**, respectively, and the onset reduction potentials (E_{red}) are -1.23 and -1.20 V for **P1** and **P2**, respectively. The highest occupied molecular orbital (HOMO) and LUMO energy levels and band gaps ($E_{g,ec}$) of polymers were calculated according to the following equations:

$$E_{HOMO} = -e(E_{ox} + 4.71) \text{ (eV)} \quad (1)$$

$$E_{LUMO} = -e(E_{red} + 4.71) \text{ (eV)} \quad (2)$$

$$E_{g,ec} = E_{ox}^{onset} - E_{red}^{onset} \text{ (eV)} \quad (3)$$

The energy levels calculated from the CV results indicated that these new polymers are good candidates as donor materials. The LUMO energy levels of **P1** and **P2** are -3.48 and -3.51 eV, which are higher than the LUMO level of PC₆₁BM (-4.1 eV), guaranteeing the photo-induced electron transfer from the donor to acceptor, that is, from polymers to PC₆₁BM. The band gap (E_g) of **P1** and **P2** calculated from the CV results is 1.85 and 1.93 eV, respectively. The optical band gaps (E_g) of **P1** and **P2** were determined from the onset of absorption to be 1.95 and 1.98 eV, respectively.

As shown in Figure 2, **P1** and **P2** displayed quite similar absorption spectra both in solutions and films. In solutions, the two polymers exhibited a broad absorption ranging from 300 to 650 nm with two peaks located at about 390 and 520 nm, respectively. Compared with the solution absorption

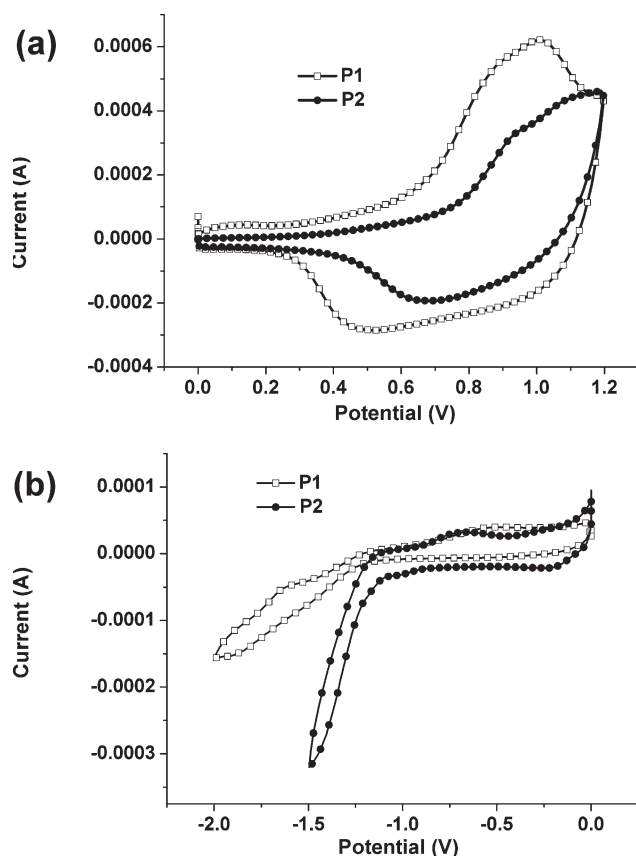


FIGURE 1 Cyclic voltammograms of polymer films in acetonitrile solution containing 0.1 M Bu_4NPF_6 and Ag/AgNO_3 as the reference electrode.

spectra, the film ones were both slightly broader and red-shifted for about 30 nm.

Mobility Test

FET mobility measurements were carried out to detect the hole mobility of the polymers. **P1** and **P2** exhibited hole mobilities of about 4.3×10^{-4} and $3.2 \times 10^{-3} \text{ cm}^2 \text{ V}^{-1} \text{ s}^{-1}$, respectively. Mobility higher than $10^{-3} \text{ cm}^2 \text{ V}^{-1} \text{ s}^{-1}$ is desired for high-efficiency PSCs having efficient carrier transport ability.¹⁸

Photovoltaic and Morphological Properties

Photovoltaic properties of **P1** and **P2** were first investigated in devices with the structure of indium tin oxides (ITO)/poly(3,4-ethylenedioxythiophen):polystyrolsulfonate (PEDOT:PSS)/active layer/LiF/Al. The active layer is a blend of polymer and PC_{61}BM . The influence of different solvent, the ratio of polymer to PC_{61}BM , the concentration of 1,8-diodooctane (DIO) additive, and the spinning speed to the photovoltaic performance was investigated in detail. The optimization process was carried out in the following order: the ratio of polymer to PC_{61}BM , the concentration of the additive, and the spinning speed. The results for **P2** are listed in Supporting Information Table S1 and their J - V curves are shown in Supporting Information Figure S1.

For **P1**, the optimized ratio of polymer to PC_{61}BM was 1:4 (w/w), the concentration of polymer is 7.5 mg mL^{-1} , the concentration of DIO in DCB is 2.5% (in volume), and the spin coating speed is 1500 rpm. The device showed a V_{oc} of 0.71 V, a J_{sc} of 4.95 mA cm^{-2} , an FF of 0.50, and a PCE of 1.78%. For **P2**, initial test results showed that devices fabricated with a ratio of polymer to PC_{61}BM of 1:3 in CB and spin-coated at a speed of 1000 rpm gave a V_{oc} of 0.87 V, a J_{sc} of 7.91 mA cm^{-2} , an FF of 0.59, and a PCE of 4.05%. The PCE of PSCs based on **P2**/ PC_{61}BM -blend films was further increased to 4.81% by using a solvent mixture of CB containing 2.5% (in volume) of DIO. When PC_{71}BM was used as the acceptor, PCEs were increased from 1.78 to 2.72% for **P1** and from 4.81 to 5.08% for **P2**. These data are also summarized in Table 1. The increase of the PCE is probably attributed to the increased J_{sc} , owing to the light absorption of PC_{71}BM in the visible region.¹⁹ The external quantum efficiency (EQE) curve of a solar cell with **P2** and PC_{71}BM as the active layer is shown in Figure 3, which ranged from 300 to 720 nm and showed a broad coverage of the solar spectrum. The photocurrent of photovoltaic cells was recorded under monochromatic illumination. The complementary absorbance of **P2** and PC_{71}BM makes the EQE higher than 50% from 350 to 600 nm and with an onset at 720 nm. It was reported that the introduction of a TiO_x thin layer as an optical spacer between the active layer and the top metal electrode can redistribute the light intensity within the active layer, shield against physical damage and chemical degradation of the active layer, and significantly increase the PCE of the photovoltaic devices.^{5,20,21} After the introduction of a TiO_x layer between the active layer and top metal electrode, the PCE of **P2** was further improved to 6.05% with a J_{sc} of 11.5 mA cm^{-2} and the J - V characteristic is shown in Figure 4.

Atomic force microscopy (AFM) images ($5 \times 5 \mu\text{m}^2$) of films spin-coated from solutions of polymer and PC_{61}BM containing different amount of DIO measured by AFM using the tapping mode are shown in Figure 5. As shown in Figure 5(a,d), blend films of **P1**: PC_{61}BM spin-coated from DCB solutions and blend films of **P2**: PC_{61}BM spin-coated from CB solutions

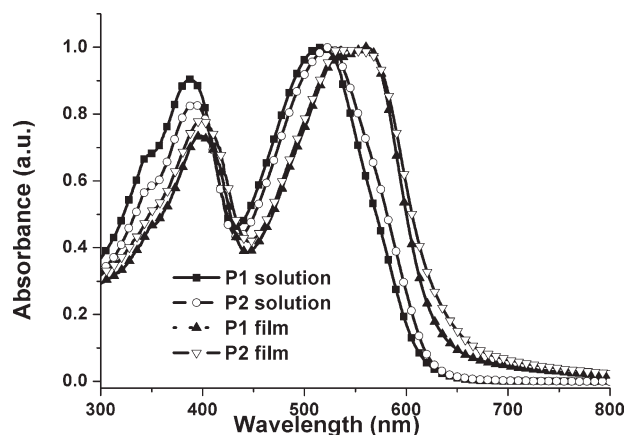


FIGURE 2 Normalized UV-vis absorption spectra of **P1** and **P2** in dilute CHCl_3 solutions and films on quartz substrates.

TABLE 1 Optimized Photovoltaic Properties of PSCs Based on **P1** and **P2**

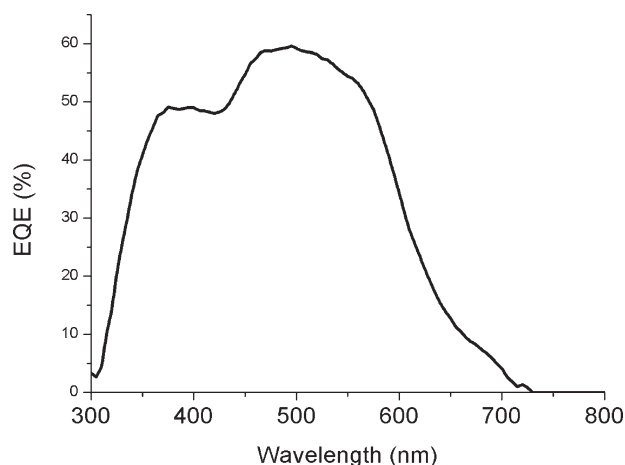
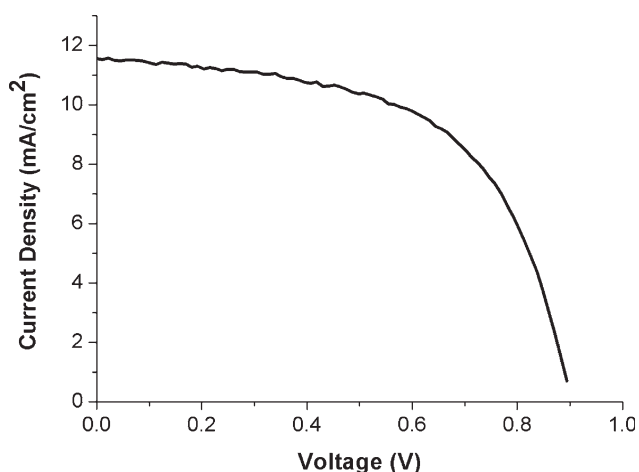
Active Layer	Additive Content (vol %)	V_{oc} (V)	TiO_x	J_{sc} ($mA\ cm^{-2}$)	FF	PCE (%)
P1 :PC ₆₁ BM = 1:4	2.5	0.71	Without	4.95	0.50	1.78
P1 :PC ₇₁ BM = 1:4	2.5	0.86	Without	5.77	0.55	2.72
P2 :PC ₆₁ BM = 1:3	2.5	0.87	Without	8.83	0.64	4.81
P2 :PC ₇₁ BM = 1:3	2.5	0.84	Without	10.67	0.59	5.08
P2 :PC ₇₁ BM = 1:3	2.5	0.91	With	11.50	0.58	6.05

displayed smooth surfaces with root-mean-square (RMS) roughness of 0.447 and 0.675 nm, respectively. Figure 5(b,e) shows AFM images of blend films spin-coated from the solutions containing 2.5% of DIO. The addition of 2.5% of DIO could significantly increase the phase separation of blend films and the RMS values were increased to 3.831 and 2.955 nm for **P1** and **P2**, respectively. Although these two blend films show similar surface topography, their phase images are quite different as shown in Figure 5(c,f). As a complement to topographic images, phase images can provide information on sample heterogeneity. From the phase image, it is easy to find that the domain size formed by phase separation of **P2**/PC₆₁BM blend film is much smaller and more uniform than that of **P1**/PC₆₁BM blend film. Appropriate and uniform domain size may favor for the efficient exciton separation and diffusion.

To deeply understand the influence of additive on the device performance, films spin-coated from **P2**/PC₆₁BM in CB containing different amount of DIO were investigated in detail. The surface topography ($2 \times 2\ \mu m^2$) of these films obtained by AFM using the tapping mode is shown in Figure 6(a–e). The morphology and domain size of blend films are very sensitive to the concentration of additive. With the increase of the concentration of DIO from 0 to 5%, RMS values increased from 0.467 to 4.953 nm, and the domain size also became larger. Devices fabricated under optimal conditions (containing

2.5% of DIO) gave the highest PCE. Only blend films spin-coated under the optimal conditions showed uniform and spheriform domains, which disappeared by either increasing or decreasing the concentration of DIO. From the above results, we can easily find that the PCE is closely related to the morphology of blend films. Only appropriate RMS number and domain size can give the best device performance.

When TiO_x spacer was used between the photo-active layer and the top electrode, it was reported that the physical defects of films could be prevented and the durability could be improved.²⁰ As shown in Figure 6(f), AFM image of blend films covered with a TiO_x layer revealed that the TiO_x layer was not a continuous and homogeneous film. It is hard for a very thin TiO_x layer to form a continuous and homogeneous film on the blend film. Hole-blocking properties of TiO_x layer were investigated by measuring the dark J - V curves of solar cells and the resulting dark current density versus bias voltage curves of **P2**:PC₇₁BM blend films covered with and without TiO_x are summarized in Figure 7. Solar cells with the TiO_x spacer displayed better rectification property and smaller leakage current than those without the TiO_x spacer. Under a negative bias of $-2\ V$, holes will be injected from Al electrode to the TiO_x layer. The relative smaller current density of the device with a TiO_x spacer indicated that the TiO_x film is an effective hole-blocking layer, which helps to improve the J_{sc} of devices.

**FIGURE 3** EQE spectrum of PSCs based on **P2**/PC₇₁BM from CB with 2.5% DIO.**FIGURE 4** Current density–voltage characteristic of PSCs based on **P2**/PC₇₁BM under AM 1.5 G illumination.

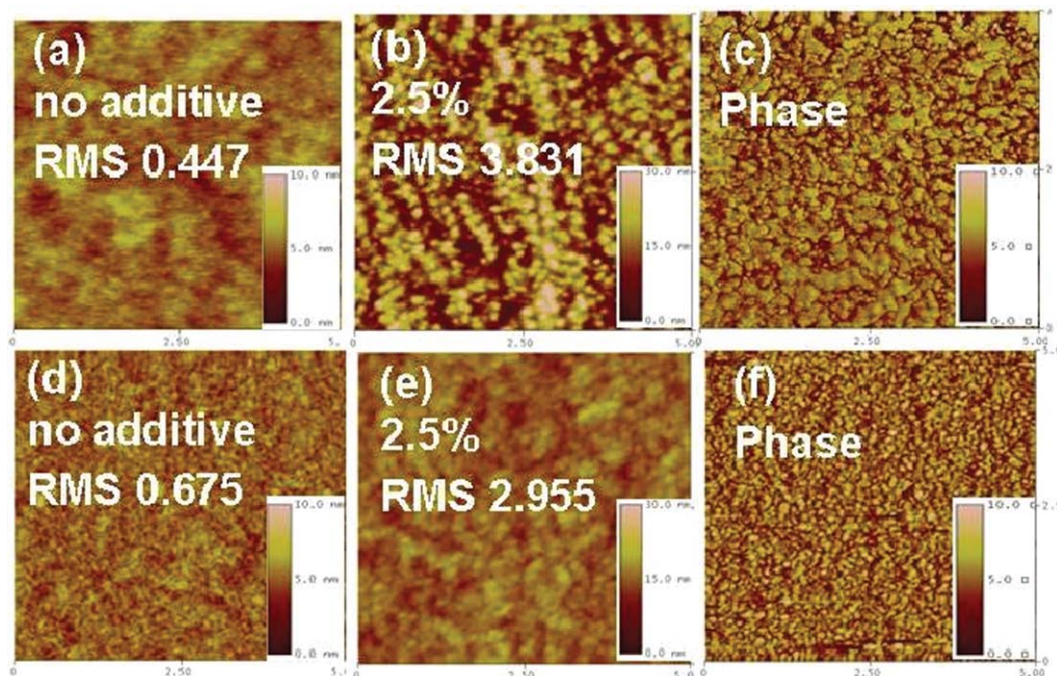


FIGURE 5 AFM topography images of **P1/PC₆₁BM** (1:4, w/w) blend films spin-coated from DCB solution (a) and DCB solution with 2.5 vol % DIO (b); phase image of **P1/PC₆₁BM** (1:4, w/w) blend films spin-coated from DCB with 2.5 vol % DIO (c); AFM topography images of **P2/PC₆₁BM** (1:3, w/w) blend films spin-coated from CB solution (d) and CB solution with 2.5 vol % DIO (e); phase image of **P2/PC₆₁BM** (1:3, w/w) blend films with 2.5 vol % DIO (f).

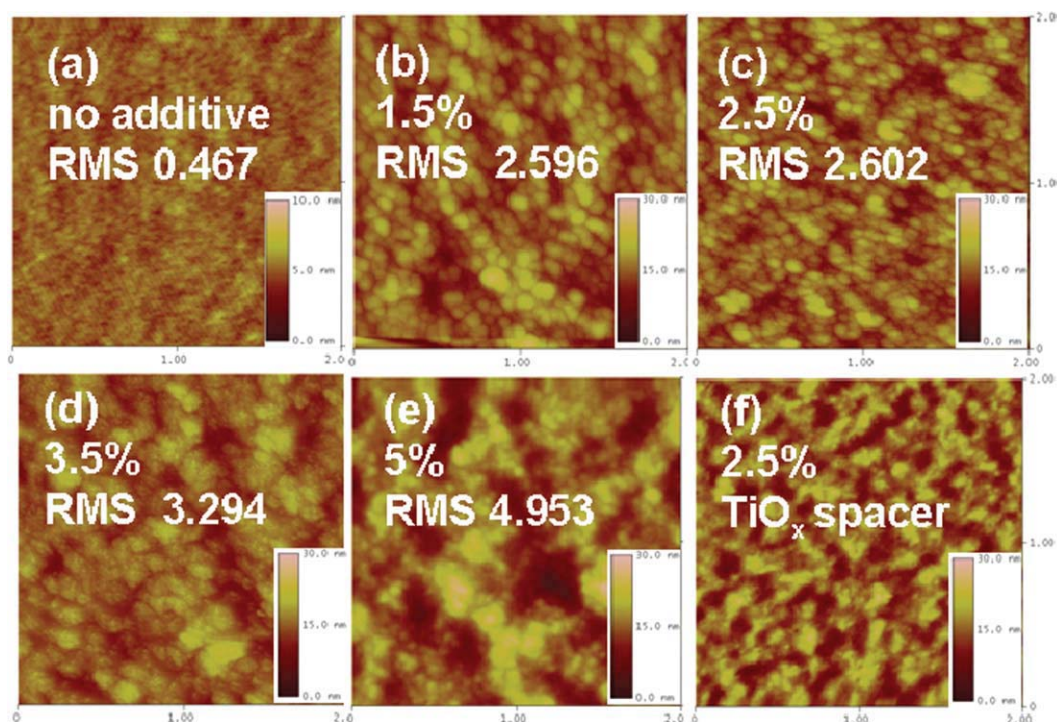


FIGURE 6 AFM topography of blend films of **P2/PC₆₁BM** (1:3, w/w) spin-coated from CB solution with different DIO concentrations (from 0 to 5 vol %; a–e). AFM topography of blend films of **P2/PC₆₁BM** (using 2.5% DIO) coated with a TiO_x film (f). [Color figure can be viewed in the online issue, which is available at wileyonlinelibrary.com.]

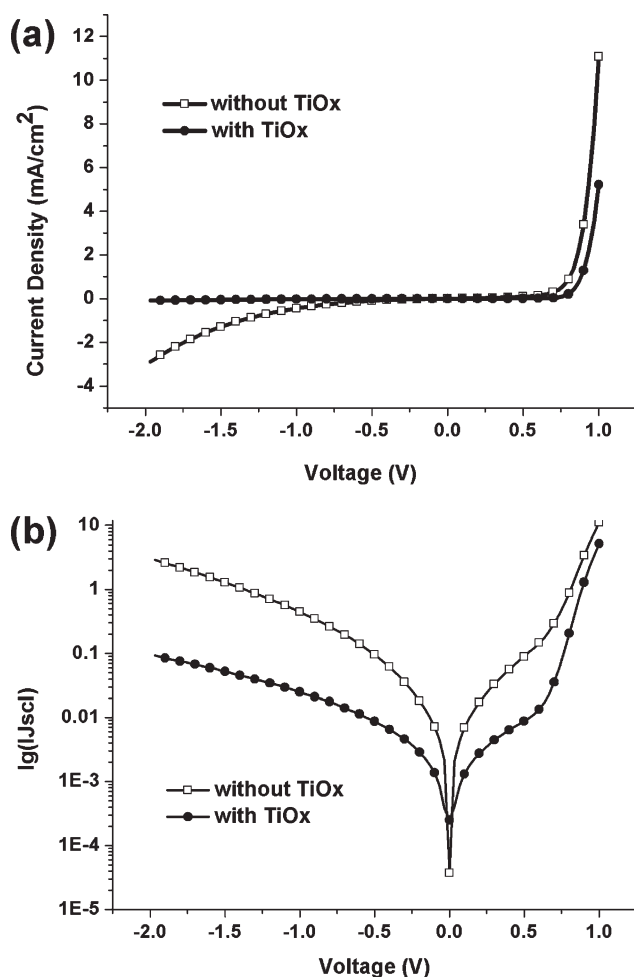


FIGURE 7 Photovoltaic properties of devices made from P2/PC₇₁BM blends with and without a TiO_x layer under dark: (a) *I*-*V* curves and (b) the absolute value of current density on log scale.

EXPERIMENTAL

Materials and Instruments

All reagents were purchased from commercial suppliers and used without further purification unless otherwise indicated. THF and toluene were distilled from Na under nitrogen with benzophenone as an indicator. Compound **1**,^{13,14} 4,7-bis(5-bromothiophen-2-yl)-5,6-bis(octyloxy)benzo[*c*][1,2,5]thiadiazole (**M1**)⁸ and 9,9-dioctyl-2,7-bis(4,4,5,5-tetramethyl-1,3,2-dioxaborolane-2-yl)dibenzosilole (**M3**)¹³ were prepared by following the literature procedures.

Thin-layer chromatography analysis was performed using silica gel HSG (F254) plates, and the eluted plates were observed under a UV detector. Chromatographic purifications were performed by flash chromatography on silica gel (200–300 mesh). ¹H and ¹³C NMR spectra were recorded on a Bruker AV400 spectrometer with chloroform-*d*₁ as the solvent. UV-vis absorption spectra were recorded on a UV-1601pc spectrometer. Elemental analysis was performed on a Vario EL elemental analysis instrument. *M_n* and weight-av-

erage molecular weights (*M_w*) were measured by GPC on a Waters GPC2410 with THF as an eluent calibrated with polystyrene standards. AFM images of blend films were obtained on a Nanoscope IIIa Dimension 3100 operating in the tapping mode. TGA was performed on a Perkin-Elmer Pyris 1 analyzer under nitrogen atmosphere (100 mL min⁻¹) at a heating rate of 10 C min⁻¹. DSC measurements were performed on a Mettler Toledo DSC 822e with a heating and cooling rate of 20 C min⁻¹. Electrochemical measurements were performed on a CHI 630A Electrochemical Analyzer.

Device Processing and Characterization

PSCs were fabricated with the device configuration of ITO/PEDOT:PSS/active layer/LiF/Al or ITO/PEDOT:PSS/active layer/TiO_x/Al. The conductivity of ITO was 20 Ω sq.⁻¹ and PEDOT:PSS is Baytron P VPAI 4083. A thin layer of PEDOT:PSS was spin-coated on the top of cleaned ITO substrate at 2,400 rpm s⁻¹ and dried subsequently at 120 °C for 10 min on a hotplate. The active layer was prepared in air by spin coating the CB or DCB solution of polymers and PC₆₁BM or PC₇₁BM on the top of ITO/PEDOT:PSS. About 1 nm of LiF was thermally evaporated or 10 nm of TiO_x was spin-coated on to the active layer, following with annealing at 80 °C for 10 min in air. The top electrode was thermally evaporated 100 nm of aluminum at a pressure of 10⁻⁴ Pa through a shadow mask. Eight organic solar cells (OSCs) were fabricated on one substrate and the effective area of one cell is 4 mm². The characterization of solar cell devices was carried out on a computer controlled Keithley 236 digital source meter with an AM 1.5 solar simulator (Oriel model 96000; 100 mW cm⁻²) as the light source.

2,7-Dibromo-9,9-dimethyldibenzosilole (Compound 2)

n-Butyllithium (6.5 cm³, 16.24 mmol, 2.5 M in hexane) was added to a solution of 4,4'-dibromo-2,2'-diiodobiphenyl (2.29 g, 4.06 mmol) in dry THF (50 cm³) at -90 °C under nitrogen atmosphere for 0.5 h. The mixture was stirred for a further 1 h at -90 °C, then dichlorodimethylsilane (1.50 cm³, 12.4 mmol) was added and the mixture was brought up to room temperature and stirred overnight. The reaction was quenched with distilled water and the mixture was then extracted with diethyl ether (100 mL). Organic layer was washed with brine (100 mL × 3), dried with anhydrous Na₂SO₄, and evaporated. On purification by column chromatography with hexane as the eluent, Compound **2** was obtained as colorless crystal (0.6 g, 40%).

¹H NMR (400 MHz, CDCl₃, δ): 0.43 (s, 6H; CH₃), 7.54 (dd, *J* = 8.3, 2H; ArH), 7.63 (d, *J* = 8.3, 2H; ArH), 7.70 (s, 2H; ArH); ¹³C NMR (100 MHz, CDCl₃, δ): -3.25, 122.61, 122.75, 133.47, 135.78, 141.64, 145.73. Anal. Calcd for C₁₄H₁₂Br₂Si: C, 45.68; H, 3.29. Found: C, 45.64; H, 3.35.

9,9-Dimethyl-2,7-bis(4,4,5,5-tetramethyl-1,3,2-dioxaborolane-2-yl)dibenzosilole (M2)

A mixture of Compound **2** (0.592 g, 1.62 mmol), 4,4,5,5-tetramethyl-2-(4,4,5,5-tetramethyl-1,3,2-dioxaborolan-2-yl)-1,3,2-dioxaborolane (1.03 g, 4.06 mmol), dry potassium acetate (1.03 g, 4.06 mmol), and dry *N,N*-dimethylformamide (DMF) (20 mL) was carefully degassed before and after Pd(dppf)Cl₂

(30 mg, 36.8 μmol) was added. The mixture was stirred at 80 $^{\circ}\text{C}$ for 2 days under nitrogen atmosphere. Then, the reaction mixture was cooled to room temperature, added with water (50 mL) and extracted with hexane (20 mL \times 3). Organic layer was washed with brine (50 mL \times 3), dried with anhydrous Na_2SO_4 , and evaporated to dryness. The residue was chromatographically purified on a silica gel column eluting with acetic ester/hexane (1:5, v/v) to afford **M2** as colorless crystal (0.56 g, 75%).

^1H NMR (400 MHz, CDCl_3 , δ): 0.42 (s, 6H; CH_3), 1.37 (s, 24H; CH_3), 7.86 (d, $J = 7.8$, 2H; ArH), 7.90 (d, $J = 7.8$, 2H; ArH), 8.10 (s, 2H; ArH); ^{13}C NMR (100 MHz, CDCl_3 , δ): -3.06, 25.05, 83.95, 120.7, 137.1, 138.8, 139.5, 150.5. Anal. Calcd for $\text{C}_{26}\text{H}_{36}\text{B}_2\text{O}_4\text{Si}$: C, 67.55; H, 7.85. Found: C, 67.66; H, 7.89.

General Procedures for the Synthesis of Polymers 1 and 2 Using Suzuki–Miyaura–Schlüter Polycondensation

A mixture of 4,7-bis(5-bromothiophen-2-yl)-5,6-bis(octyloxy)benzo[*c*]-[1,2,5]thiadiazole (**M1**), 9,9-dialkyl-2,7-bis(4,4,5,5-tetramethyl-1,3,2-dioxaborolane-2-yl)dibenzosilole (**M2** or **M3**), NaHCO_3 (0.6 g, 71.4 mmol), H_2O (3 mL), toluene (20 mL), and THF (8 mL) was carefully degassed before and after 3 mg $\text{Pd}(\text{PPh}_3)_4$ was added. The mixture was stirred and refluxed for 1 week under nitrogen atmosphere. Phenylboronic acid (10 mg, 0.08 mmol) was added; the reaction was further refluxed for 1 day; then 1-bromobenzene (0.05 mL, 0.48 mmol) was added and the reaction was refluxed for another 1 day. The reaction mixture was then allowed to cool to room temperature, the whole reaction mixture was poured into acetone (200 mL), and the resulted precipitate was collected by filtration. The crude polymer was dissolved in chloroform (200 mL) and filtered. The filtration was concentrated to about 80 mL and precipitated into acetone (300 mL). The precipitate was collected by filtration and dried under high vacuum to afford the aimed polymer.

Poly(4-(5-(9,9-dimethyl-9H-dibenzosilole-2-yl)thiophen-2-yl)-5,6-bis(octyloxy)-7-(thiophen-2-yl)benzo[*c*][1,2,5]-thiadiazole) (P1)

M1 (100 mg, 0.140 mmol) and **M2** (64.4 mg, 0.139 mmol) were used. **P1** was obtained as dark solid (90 mg, 84%). M_n and PDI measured by GPC calibrated with polystyrene standards are 79.8 kg mol^{-1} and 1.46, respectively.

^1H NMR (400 MHz, CDCl_3 , δ): 8.54 (br, 2H), 8.00–7.75 (mbr, 6H), 7.51 (br, 2H), 4.21 (br, 4H), 2.09 (br, 4H), 1.54–1.26 (mbr, 20H), 0.89 (br, 6H), 0.56 (br, 6H); ^{13}C NMR (100 MHz, CDCl_3 , δ): 151.83, 150.94, 133.40, 133.39, 131.97, 130.10, 130.06, 127.88, 121.36, 117.54, 74.55, 74.53, 31.92, 31.86, 30.54, 30.06, 29.69, 29.64, 29.52, 29.48, 29.33, 26.11, 22.90, 22.68, 14.27, 14.16, 14.11, -3.12. Anal. Calcd for $(\text{C}_{44}\text{H}_{52}\text{N}_2\text{O}_2\text{S}_3\text{Si})_n$: C, 69.07; H, 6.85; N, 3.66. Found: C, 67.98; H, 6.57; N, 3.42.

Poly(4-(5-(9,9-dioctyl-9H-dibenzosilole-2-yl)thiophen-2-yl)-5,6-bis(octyloxy)-7-(thiophen-2-yl)benzo[*c*][1,2,5]-thiadiazole) (P2)

M1 (100 mg, 0.140 mmol) and **M3** (91.7 mg, 0.139 mmol) were used. **P2** was obtained as dark solid (120 mg, 90%).

M_n and PDI measured by GPC calibrated with polystyrene standards are 102.0 kg mol^{-1} and 1.66, respectively.

^1H NMR (400 MHz, CDCl_3 , δ): 8.57 (br, 2H), 8.00–7.82 (mbr, 6H), 7.53 (br, 2H), 4.21 (br, 4H), 2.03 (br, 4H), 1.54–0.84 (mbr, 60H); ^{13}C NMR (100 MHz, CDCl_3 , δ): 151.82, 150.98, 147.47, 145.91, 139.04, 133.60, 133.21, 132.14, 131.98, 132.14, 132.08, 131.99, 130.48, 128.78, 128.46, 127.78, 127.06, 122.97, 121.36, 121.23, 117.56, 74.53, 33.45, 33.41, 31.88, 30.58, 29.70, 29.67, 29.54, 29.38, 29.26, 29.22, 29.14, 29.11, 26.14, 24.01, 22.81, 22.71, 22.65, 14.22, 14.12, 14.09. Anal. Calcd for $(\text{C}_{58}\text{H}_{80}\text{N}_2\text{O}_2\text{S}_3\text{Si})_n$: C, 72.45; H, 8.39; N, 2.91. Found: C, 69.28; H, 8.03; N, 2.59.

CONCLUSIONS

In conclusion, low-band gap conjugated polymers (**P1** and **P2**) with a dibenzosilole–thiophene–benzothiadiazole–thiophene main chain were synthesized and used for PSCs. These two polymers are of high molecular weight and good solubility in commonly used organic solvents. PSCs were fabricated with the blends of polymers and PC_{71}BM as the active layer. PCEs of the optimized photovoltaic cells are 2.72% for **P1** and 5.08% for **P2** under the illumination of AM 1.5 (100 mW cm^{-2}). The performances of solar cells based on **P2** were further increased to 6.05% for PCE, 0.91 V for V_{oc} , 11.50 mA cm^{-2} for J_{sc} and 0.58 for FF, indicating that **P2** is a promising donor material for solar cell applications.

Financial support by the NSF of China (50603027 and 20834006), the 863 Program (2008AA05Z425), and the 973 Program (2009CB623601) is gratefully acknowledged.

REFERENCES AND NOTES

- Chen, H.; Hou, J.; Zhang, S.; Liang, Y.; Yang, G.; Yang, Y.; Yu, L.; Wu, Y.; Li, G. *Nat Photonics* 2009, 3, 649–653.
- Liang, Y.; Xu, Z.; Xia, J.; Tsai, S.-T.; Wu, Y.; Li, G.; Ray, C.; Yu, L. *Adv Mater* 2010, 22, E135–E138.
- Peet, J.; Kim, J. Y.; Coates, N. E.; Ma, W. L.; Moses, D.; Heeger, A. J.; Bazan, G. C. *Nat Mater* 2007, 6, 497–500.
- Hou, J. H.; Chen, H. Y.; Zhang, S. Q.; Li, G.; Yang, Y. *J Am Chem Soc* 2008, 130, 16144–16145.
- Park, S. H.; Roy, A.; Beaupre, S.; Cho, S.; Coates, N.; Moon, J. S.; Moses, D.; Leclerc, M.; Lee, K.; Heeger, A. J. *Nat Photonics* 2009, 3, 297–302.
- Hou, J.; Chen, H.-Y.; Zhang, S.; Chen, R. I.; Yang, Y.; Wu, Y.; Li, G. *J Am Chem Soc* 2009, 131, 15586–15587.
- Liang, Y.; Feng, D.; Wu, Y.; Tsai, S.-T.; Li, G.; Ray, C.; Yu, L. *J Am Chem Soc* 2009, 131, 7792–7799.
- Qin, R. P.; Li, W. W.; Li, C. H.; Du, C.; Veit, C.; Schleiermacher, H. F.; Andersson, M.; Bo, Z. S.; Liu, Z. P.; Inganäs, O.; Wuerfel, U.; Zhang, F. L. *J Am Chem Soc* 2009, 131, 14612–14613.
- Chen, H. Y.; Hou, J. H.; Hayden, A. E.; Yang, H.; Hou, K. N.; Yang, Y. *Adv Mater* 2010, 22, 371–375.
- Zou, Y. P.; Najari, A.; Berrouard, P.; Beaupre, S.; Aich, B. R.; Tao, Y.; Leclerc, M. *J Am Chem Soc* 2010, 132, 5330–5331.
- Huo, L. J.; Hou, J. H.; Zhang, S. Q.; Chen, H. Y.; Yang, Y. *Angew Chem Int Ed* 2010, 49, 1500–1503.

- 12** Scharber, M. C.; Koppe, M.; Gao, J.; Cordella, F.; Loi, M. A.; Denk, P.; Morana, M.; Egelhaaf, H.-J.; Forberich, K.; Dennler, G.; Gaudiana, R.; Waller, D.; Zhu, Z.; Shi, X.; Brabec, C. J. *Adv Mater* 2010, 22, 367–370.
- 13** Chan, K. L.; McKiernan, M. J.; Towns, C. R.; Holmes, A. B. *J Am Chem Soc* 2005, 127, 7662–7663.
- 14** Usta, H.; Lu, G.; Facchetti, A.; Marks, T. J. *J Am Chem Soc* 2006, 128, 9034–9035.
- 15** Tamao, K.; Uchida, M.; Izumizawa, T.; Furukawa, K.; Yamaguchi, S. *J Am Chem Soc* 1996, 118, 11974–11975.
- 16** Wang, E. G.; Wang, L.; Lan, L. F.; Luo, C.; Zhuang, W. L.; Peng, J. B.; Cao, Y. *Appl Phys Lett* 2008, 92, 033307/1–033307/3.
- 17** Boudreault, P. L. T.; Michaud, A.; Leclerc, M. *Macromol Rapid Commun* 2007, 28, 2176–2179.
- 18** Scharber, M. C.; Mühlbacher, D.; Koppe, M.; Denk, P.; Waldauf, C.; Heeger, A. J.; Brabec, C. J. *Adv Mater* 2006, 18, 789–794.
- 19** Wienk, M. M.; Kroon, J. M.; Verhees, W. J. H.; Knol, J.; Hummelen, J. C.; Hal, P. A. V.; Janssen, R. A. J. *Angew Chem Int Ed* 2003, 42, 3371–3375.
- 20** Hayakawa, A.; Yoshikawa, O.; Fujieda, T.; Uehara, K.; Yoshikawaa, S. *Appl Phys Lett* 2007, 90, 163517/1–163517/3.
- 21** Kim, J. Y.; Kim, S. H.; Lee, H. H.; Lee, K.; Ma, W. L.; Gong, X.; Heeger, A. J. *Adv Mater* 2006, 18, 572–576.